PHYSICAL REVIEW E **89**, 012501 (2014)

Effect of a bias electric field on the structure and dielectric response of the ferroelectric smectic-*A* liquid crystal in thin planar cells

K. Gornik,[1] M. Čepič,[2,3] and N. Vaupotič[1,3]
[1]*Department of Physics, Faculty of Natural Sciences and Mathematics, University of Maribor, Koroška cesta 160, SI-2000 Maribor, Slovenia*
[2]*Department of Physics and Technical Studies, Faculty of Education, University of Ljubljana,*
Kardeljeva ploščad 16, SI-1000 Ljubljana, Slovenia
[3]*Jozef Stefan Institute, Jamova 39, SI-1000 Ljubljana, Slovenia*

(Received 20 September 2013; revised manuscript received 30 November 2013; published 2 January 2014)

The phenomenological continuum model is used to study the director structure and dielectric response of the ferroelectric smectic-*A* phase in thin planar cells. The frequency of the phase mode and the dielectric permittivity are calculated numerically as a function of the bias external DC electric field, cell thickness, the strength of polar surface anchoring, and the ratio between the bend and splay elastic constants. The theoretically obtained dependencies are in agreement with the recently reported experimental measurements, which show that in thin planar cells both the phase mode frequency and the dielectric permittivity decrease with increasing external bias electric field.

DOI: 10.1103/PhysRevE.89.012501 PACS number(s): 61.30.Gd, 77.84.−s

I. INTRODUCTION

Liquid crystals made of bent-core molecules were discovered almost two decades ago [1]. Due to the specific shape of the molecules they tend to form polar smectic layers. In bent-core liquid crystals the polar order is decoupled from the tilt order [2–4], so smectic layers can be polar even without the long molecular axes being tilted with respect to the smectic layer normal. Because of that, ferroelectric and antiferroelectric phases are possible also in the smectic-*A*-type (Sm-*A*) phases, as opposed to the rod-like ferroelectric LCs, where polar structures are possible only in the smectic-*C* (Sm-*C*) phase. Smectic phases formed by bent-core molecules usually have an antiferroelectric interlayer structure [5,6] and until 2011 the ferroelectric interlayer structure (in the absence of external DC field) was observed only in the Sm-*C*-type phases. A ferroelectric Sm-*A* phase, which presents the highest symmetry layered ferroelectric possible, was, for a long time, only a theoretical possibility. The crucial problem was to synthesize such molecules that would promote parallel alignment of dipoles in the neighboring smectic layers. Finally, a ferroelectric property of a smectic-*A* phase consisting of bent-core molecules was discovered in 2011 [7]. The ferroelectric structure is stabilized by a silane group on one terminal chain of an asymmetric bent-core molecule.

The ferroelectric Sm-*A* phase (Sm-AP_F) made of bent-core molecules with carbosilane terminal group is the highest symmetry ferroelectric material found to date and as such extremely interesting. Its ferroelectricity was confirmed by the optical second-harmonic generation activity in the absence of an external electric field, the ferroelectric response, and high dielectric strength [8]. The properties of the Sm-AP_F phase were studied in planar cells of thicknesses from 1.6 to 25 μm. The dielectric response increases and the relaxation frequency decreases with increasing cell thickness. Such behavior was successfully explained by a continuum phenomenological model, by which the liquid crystal structure in the cell is obtained by minimization of a free energy, which contains an elastic, electrostatic, and surface contribution. The relaxation frequency and the dielectric strength were calculated, in zero bias field, as a function of cell thickness and strength of polar surface anchoring. Comparison between the experimentally obtained and modeled dependencies show that the polar surface anchoring should be very strong. This is an expected result, because spontaneous polarization in bent-core liquid crystals is very high ($\approx$300 nC/cm^2 in the Sm-AP_F phase [7–9]), so the interaction between the surface and liquid crystal molecules should be very strong. In Ref. [8] the effect of the bias DC electric field on the relaxation frequency and the dielectric response is reported, as well. Measurements show that there are (at least) two modes present. The frequency of the lower frequency mode decreases with increasing bias DC field, while the frequency of the higher frequency mode increases with increasing bias field. What comes as a surprise is that the dielectric permittivity of the lower frequency mode decreases with increasing bias field, although the relaxation frequency decreases (see Fig. 6 in Ref. [8]). The explanation of this phenomena (which differs significantly from the typical behavior observed in ferroelectric bent-core LC phases [10,11], where the relaxation frequency increases with increasing electric field and the dielectric response decreases) remained open.

In this paper we present a continuum phenomenological model to discuss in detail the effect of the DC bias field on the structure and the dielectric response of the Sm-AP_F phase in thin planar cells as a function of cell thickness, surface anchoring strength, and magnitudes of the bend and splay elastic constants. The paper is structured as follows. In Sec. II we present the theoretical model and discuss equilibrium structure in thin cells as a function of the above-mentioned parameters. In Sec. III we study the dielectric response. We focus on the low-frequency mode, which is attributed to the fluctuations in the polar director, and we show that the numerically obtained results for the relaxation frequency and dielectric permittivity agree with the experimental measurements reported in Ref. [8].

II. THEORETICAL MODEL

The cell geometry is shown in Fig. 1. Surfaces lie in the *yz* plane. The cell thickness is *L*. The average direction of

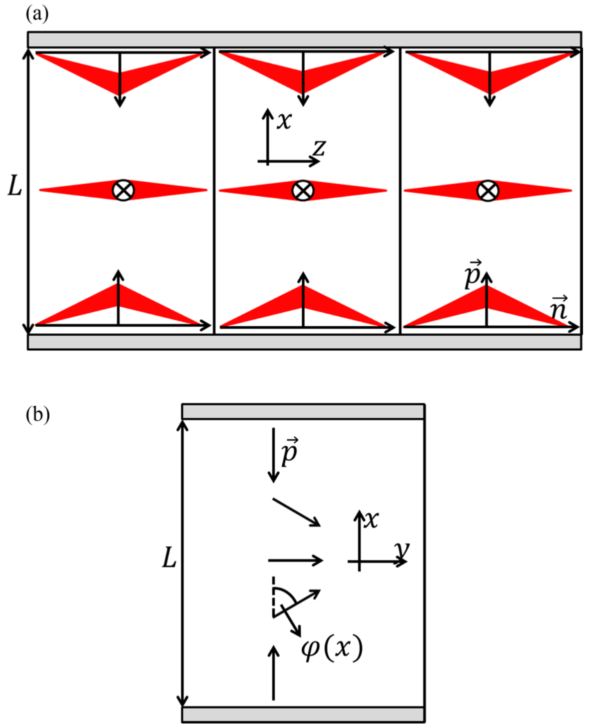

FIG. 1. (Color online) The cell geometry. L is the cell thickness, $\vec{n}$ is the director pointing along the average direction of the long molecular axes, and $\vec{p}$ is the polar director, which points in the direction of the short axes and also in the direction of the local polarization. (a) $\vec{n}$ and $\vec{p}$ director profiles in the xz plane. (b) The polar director profile in the xy plane. $\varphi(x)$ is an angle between the x axis and $\vec{p}$.

the long molecular axes is labeled with the director $\vec{n}$ and the direction of the short axes with the polar director $\vec{p}$. We assume that the smectic order parameter is constant. The director $\vec{n}$ is also constant, only the polar director $\vec{p}$ varies across the cell. We also assume that the spatial variation of the polar director is the same in all smectic layers.

The spatial variation of $\vec{p}$ is determined by a competition among the torques due to the bulk elasticity, electrostatic effects, and surface anchoring. The free energy (F) of the liquid crystal inside the cell is expressed as a sum of the bulk and surface contribution,

$$F = \int f dV + \int f_S dS, \tag{1}$$

where f is the bulk free energy density, f_S is the surface energy density, and V and S are the cell volume and surface, respectively.

The bulk free energy density is expressed as a sum of elastic and electrostatic contributions:

$$\begin{aligned} f = {} & \frac{1}{2}K_{pS}[\vec{p}\cdot(\vec{\nabla}\cdot\vec{p})]^2 + \frac{1}{2}K_{pB}[\vec{p}\times(\vec{\nabla}\times\vec{p})]^2 \\ & + \frac{P_0^2 p_x^2}{2\varepsilon\varepsilon_0} - E_B P_0 p_x, \end{aligned} \tag{2}$$

where $\vec{p} = (p_x, p_y, 0)$ and $|\vec{p}| = 1$. More conveniently, the polar director can be expressed by an angle φ [see Fig. 1(b)] as

$$\vec{p} = (\cos\varphi, \sin\varphi, 0)\,. \tag{3}$$

P_0 is the magnitude of the polarization, ε is the static dielectric constant, K_{pS} is the polarization splay, and K_{pB} is the polarization bend elastic constant. In the studied geometry there is no twist elasticity. The third term in Eq. (2) presents the self-electrostatic energy due to the permanent dipole moments and it is of crucial importance in cells when surfaces tend to enforce specific orientation of polarization [12,13]. The last term presents coupling of polarization with the external DC bias electric field (E_B), applied along the x direction.

The equilibrium structure of the polar director in the cell depends on the type and strength of surface anchoring [14]. We consider only polar surface anchoring. Polarization at the bottom and upper surfaces tends to point in the opposite directions, and the surface energy (f_S) is expressed as

$$f_S = -W_S p_x|_{(x=0)} + W_S p_x|_{(x=L)}, \tag{4}$$

where W_S is the strength of the polar surface anchoring.

The equilibrium spatial dependence of the polar director is found by minimization of the free energy [Eq. (1)]. For the purpose of numerical calculations the free energy is transformed into a dimensionless form. We introduce a correlation length,

$$\xi = \sqrt{\frac{K_{pS}\varepsilon\varepsilon_0}{P_0^2}}, \tag{5}$$

and dimensionless parameters,

$$\tilde{x} = \frac{x}{L}, \quad \tilde{E}_B = \frac{E_B\varepsilon\varepsilon_0}{P_0}, \quad \kappa = \frac{K_{pB}}{K_{pS}}, \quad \tilde{W}_S = \frac{W_S\xi}{K_{pS}}, \tag{6}$$

and define the dimensionless free energy ($\tilde{F}$) as

$$\tilde{F} = \frac{L}{K_{pS}}F = \int_0^1 \tilde{f}\, d\tilde{x} + \tilde{F}_S, \tag{7}$$

where the dimensionless bulk free energy density ($\tilde{f}$) is

$$\begin{aligned} \tilde{f} = {} & \frac{1}{2}\left(\frac{dp_x}{d\tilde{x}}\right)^2 + \frac{1}{2}\kappa\left(\frac{dp_y}{d\tilde{x}}\right)^2 \\ & + \frac{1}{2}\left(\frac{L}{\xi}\right)^2 p_x^2 - \left(\frac{L}{\xi}\right)^2 \tilde{E}_B p_x, \end{aligned} \tag{8}$$

and the dimensionless surface free energy density ($\tilde{f}_S$) is

$$\tilde{f}_S = -\tilde{W}_S\left(\frac{L}{\xi}\right) p_x\Big|_{x=0} + \tilde{W}_S\left(\frac{L}{\xi}\right) p_x\Big|_{x=L}. \tag{9}$$

We refrain from using a one-constant approximation ($K_{pB} = K_{pS}$), because in the bent-core liquid crystals the bend elastic constant is much lower than the splay elastic constant [15–18] (in rod-like LC, on the other hand, the bend elastic constant is always the largest [19]). We have to point out that the elastic constants measured in Refs. [15–18,20] are the bend and splay elastic constants in the deformation of the director $\vec{n}$, while this model includes elastic constants for the splay and bend deformation of the short molecular axis. However, for the elastic deformations in the short axis the splay elastic constant can also be expected to be larger than the bend elastic constant as deduced from the defect structure in Sm-AP_F (see Fig. 3(G) in Ref. [7]). Still, we decided to keep the ratio κ as a parameter and study the structure and the dielectric response also as a function of parameter κ.

Minimization of the free energy over the angle φ gives the Euler-Lagrange equation

$$\frac{\partial \tilde{f}}{d\varphi} - \frac{d}{d\tilde{x}} \frac{\partial \tilde{f}}{\partial\,(d\varphi/d\tilde{x})} = 0 \tag{10}$$

and two boundary conditions

$$\left[\pm \frac{\partial \tilde{f}}{\partial(d\varphi/d\tilde{x})} + \frac{\partial \tilde{f}_S}{\partial\varphi}\right]_{x=0,L} = 0, \tag{11}$$

where the positive sign is valid at $x = L$ and the negative sign at $x = 0$.

Using the relation Eq. (3) between the polar director $\vec{p}$ and angle φ and inserting the dimensionless free-energy densities [Eqs. (8) and (9)] into Eqs. (10) and (11) leads to the following bulk equation:

$$(\sin^2\varphi + \kappa\cos^2\varphi)\frac{d^2\varphi}{d\tilde{x}^2} + \frac{1}{2}(1-\kappa)\sin 2\varphi\left(\frac{d\varphi}{d\tilde{x}}\right)^2 + \frac{1}{2}\left(\frac{L}{\xi}\right)^2 \sin 2\varphi - \tilde{E}_B\left(\frac{L}{\xi}\right)^2 \sin\varphi = 0, \tag{12}$$

and two surface equations

$$\left[\tilde{W}_S\left(\frac{L}{\xi}\right)\sin\varphi + (\sin^2\varphi + \kappa\cos^2\varphi)\frac{d\varphi}{d\tilde{x}}\right]_{x=0,L} = 0. \tag{13}$$

Equations (12) and (13) are solved numerically for the variable $\varphi(x)$ at different values of the parameters κ, $\tilde{W}_S$, $\tilde{E}_B$, and L/ξ. The results of numerical calculation are presented below.

A. The polar director profile in bias electric field

In Fig. 2 we show spatial variation of the x component of the polar director $\vec{p}$ across the cell for different strengths of polar surface anchoring. The director profile is calculated at $\kappa = 0.3$ and $L/\xi = 7$. If κ is increased, the spatial variation of p_x close to the surfaces, where the bend deformation is the largest [see Fig. 1(b)], flattens (see Fig. 3). The effect of κ on the spatial variation of the polar director in very thin cells ($L/\xi \sim 1$) and strong polar surface anchoring is shown in Fig. 3. At a very small κ the polar director profile is almost linear in p_x, while at $\kappa = 1$ the profile is linear in φ, a result well known already from the one-constant approximation of the ferroelectric smectic-C phase made of rod-like molecules [21,22]. In the case of ferroelectric liquid crystals made of rod-like molecules, the spatial distortion is in the nematic director $\vec{n}$, which rotates on the cone from one surface to another. In our case the nematic director is uniform and the polar director rotates; however, mathematically the situations are identical.

If the surface anchoring strength decreases, the value of p_x at the surface [$p_x(0)$] decreases from 1 toward 0 (or increases from -1 toward 0 at the other surface) and the structure becomes more uniform. Figure 2(b) shows $p_x(0)$ as a function of $\tilde{W}_S$. The results show that in thinner cells stronger anchoring is required to orient polarization at the surfaces in the direction perpendicular to the surface. In what follows, we refer to the anchoring as strong if, in zero bias field, $p_x(0) > 0.9$, if $p_x(0) < 0.5$ we refer to the anchoring as weak and at all other values as intermediate anchoring.

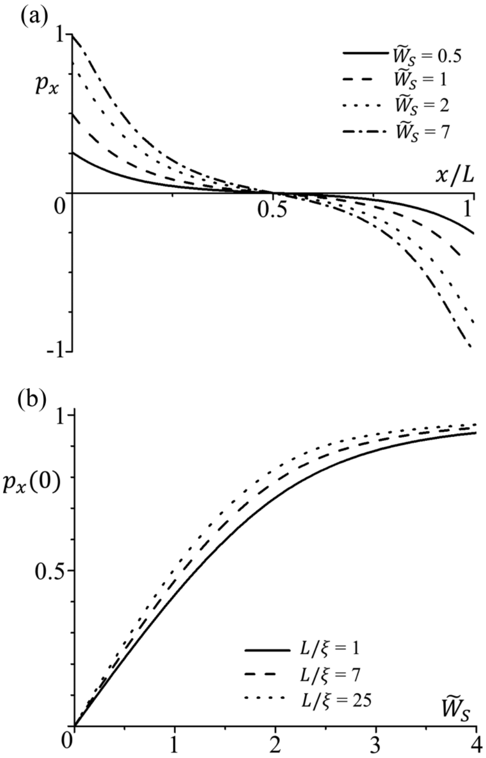

FIG. 2. (a) Spatial variation of the x component of the polar director (p_x) across the cell at different surface anchorings ($\tilde{W}_S$) at $L/\xi = 7$. (b) The value of p_x at the surface [$p_x(0)$] as a function of the polar anchoring strength $\tilde{W}_S$ at different cell thicknesses L/ξ. In all cases $\kappa = 0.3$.

Figure 4 shows the effect of the bias electric field on the polar director structure at different strengths of surface anchoring. As expected, at a given value of the bias field the reorientation of the polar director along the external field direction is stronger at weaker surface anchoring. When the bias field increases, the average value of the x component of

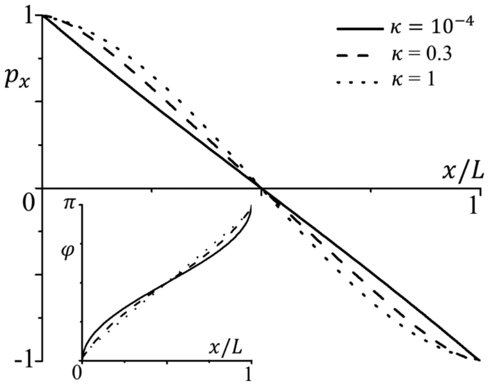

FIG. 3. Spatial variation of p_x across the cell at different κ at $L/\xi = 1$ and infinitely strong polar anchoring. Inset: Spatial variation of φ.

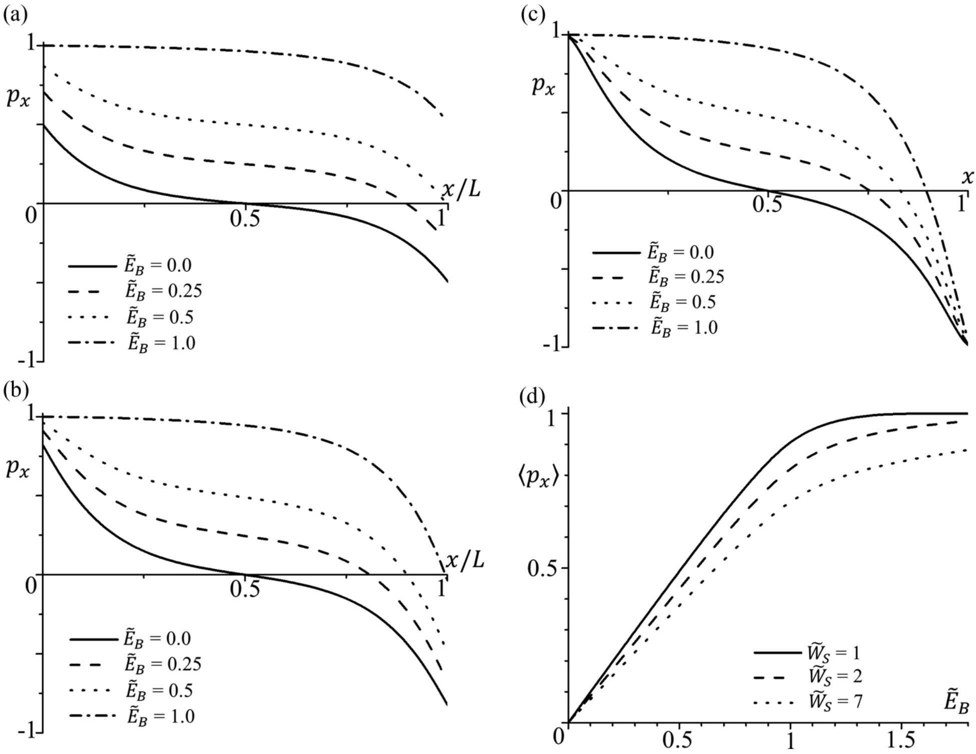

FIG. 4. Spatial variation of the x component of the polar director (p_x) across the cell at different values of the bias field $\tilde{E}_B$ at (a) weak ($\tilde{W}_S = 1$); (b) intermediate ($\tilde{W}_S = 2$); and (c) strong ($\tilde{W}_S = 7$) surface anchoring. Parameter values: $L/\xi = 7$ and $\kappa = 0.3$. (d) The average value of the x component of the polar director $\langle p_x \rangle$ as a function of the bias field $\tilde{E}_B$ at different values of surface anchoring $\tilde{W}_S$.

the polar director

$$\langle p_x \rangle = \int_0^1 p_x d\tilde{x} \tag{14}$$

increases linearly as molecular dipoles rotate toward the external field direction [Fig. 4(d)]. At weaker polar surface anchoring a uniform structure of polar director ($\langle p_x \rangle \approx 1$) is obtained at lower bias field because the surface torque, at the surface that prefers p_x in the opposite direction to the direction preferred by the bias field, is smaller.

III. THE DIELECTRIC RESPONSE

In the lower frequency region below several MHz, two collective fluctuations were detected in the SmAP$_F$ phase in thin cells [8]. The higher-frequency mode was attributed to the fluctuations in the magnitude of the local polarization (amplitude mode) and the lower frequency mode to the fluctuations in the polarization direction (phase mode). It was observed that both the phase mode relaxation frequency and the dielectric permittivity decrease with increasing bias field. In a bulk sample a decrease in relaxation frequency essentially leads to an increase in the dielectric permittivity [10,11], so the observed effect must be a result of the LC confinement.

Phase fluctuations in the polarization can be described by the fluctuations in the polar director orientation. The fluctuation of the polar director [$\delta\vec{p}(x)$] in the cell must be perpendicular to $\vec{p}(x)$ at a given position x in the cell (Fig. 5). If the AC field used for the dielectric measurements is applied along the x direction, we detect the change in the magnitude of the x component of polarization.

A. Numerical approach

To find the relaxation frequency and the magnitude of the dielectric response at the relaxation frequency we use the following method. First, we find the equilibrium polar

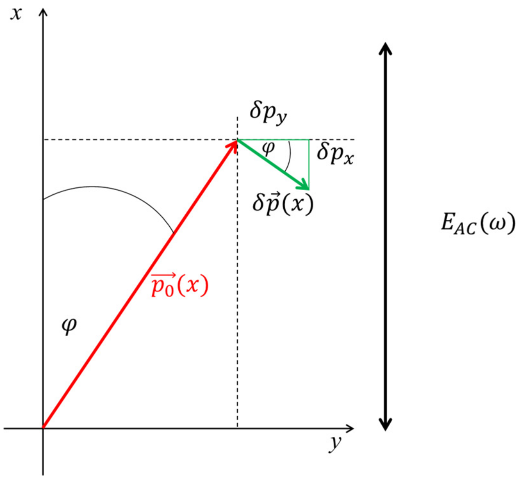

FIG. 5. (Color online) External electric field E_{AC} with frequency ω, applied along the x axis, causes fluctuations in the direction of the polar director; $\vec{p}_0(x)$ is equilibrium direction of the polar director at position x in the cell in external bias field; $\delta\vec{p}(x)$ is the fluctuation part of the polar director.

director profile in the external bias field E_B (see, for example, Fig. 4). Next, we calculate the equilibrium structure for a slightly larger electric field $E_B + \Delta E$, with $\Delta E \ll E_B$. Then we switch off ΔE and study a time-dependent relaxation of the director profile back to the equilibrium state at E_B by using the Landau-Khalatnik equation,

$$-\gamma \frac{\partial \varphi(x,t)}{\partial t} = \frac{\partial f}{\partial \varphi} - \frac{d}{dx} \frac{\partial f}{\partial (d\varphi/dx)}, \tag{15}$$

where γ is a rotational viscosity. This equation is transformed into a dimensionless version,

$$\frac{\partial \varphi(\tilde{x},\tilde{t})}{\partial \tilde{t}} = \frac{\partial \tilde{f}}{\partial \varphi} - \frac{d}{d\tilde{x}} \frac{\partial \tilde{f}}{\partial (d\varphi/d\tilde{x})}, \tag{16}$$

where a dimensionless time $\tilde{t}$ is defined as

$$\tilde{t} = t \frac{K_{pS}}{\gamma L^2}. \tag{17}$$

At the moment when ΔE is switched off, the departure of φ from the equilibrium value at a given position in the cell is $\Delta\varphi_0(x) = \varphi(x, E_B + \Delta E) - \varphi(x, E_B)$. This value decreases exponentially with time so, at some time t after ΔE was switched off, the departure of φ from the equilibrium value at field E_B is

$$\Delta\varphi(x,\tilde{t}) = \Delta\varphi_0(x)\, e^{-\tilde{t}/\tau}, \tag{18}$$

where τ is a dimensionless characteristic relaxation time. From $\Delta\varphi(x,\tilde{t})$ we obtain the relaxation time τ and assume that the relaxation frequency ω (the phase mode frequency) is inversely proportional to the relaxation time: $\omega \propto 1/\tau$.

To find the real part of the dielectric permittivity (ε') as a function of bias field at the relaxation frequency we assume that it is proportional to the value of the dielectric permittivity in the limit of a very small frequency of the AC field ($\omega_{\mathrm{AC}} \to 0$). In bulk, the dielectric permittivity at the relaxation frequency is half of the value at $\omega_{\mathrm{AC}} \to 0$, but because we are in thin cells, such an approximation is not necessarily valid. However, since the theoretically obtained dependencies of $\omega(E_B)$ and $\varepsilon'(E_B)$ agree well with the ones obtained experimentally (see Sec. III C), we conclude that the approximation can be used.

The dielectric permittivity $[\varepsilon'(E_B)]$ at $\omega_{\mathrm{AC}} \to 0$ is proportional to the change in the x component of polarization, i.e., to the increase in the x component of the polar director. Because this change varies across the cell, we calculate the average value

$$\langle \Delta p_x \rangle = \int_0^1 \Delta p_x d\tilde{x}, \tag{19}$$

where Δp_x is a difference between $p_x(E_B + \Delta E)$ and $p_x(E_B)$ at position x in the cell.

Figure 6 shows the dependence of the dielectric permittivity $\varepsilon'(E_B)$ and the relaxation frequency $\omega(E_B)$ on the magnitude of the external bias field. Relative changes with respect to the values in zero bias field [$\varepsilon'(0)$ and $\omega(0)$] are shown. Both $\varepsilon'(E_B)$ and $\omega(E_B)$ decrease with increasing bias field. However, at high bias fields the theoretically calculated $\omega(E_B)$ starts to increase while the dielectric permittivity continues to decrease.

Let us first focus on the dielectric permittivity. As already mentioned, only the variation in the x component of polarization contributes to the dielectric response. With increasing bias field the x component of polarization increases across the cell (except close to the surface at $x = L$, if anchoring is strong). At some value of the bias field, p_x close to the surface at $x = 0$ becomes uniform and equal to 1. The width of the region over which $p_x \approx 1$ increases with increasing bias field (see Fig. 4). Within this region the external AC field used in the dielectric measurements does not induce significant fluctuations of the polar director. So, the volume of the cell, which responds to the external AC field, reduces with increasing bias field and as a result the dielectric response decreases.

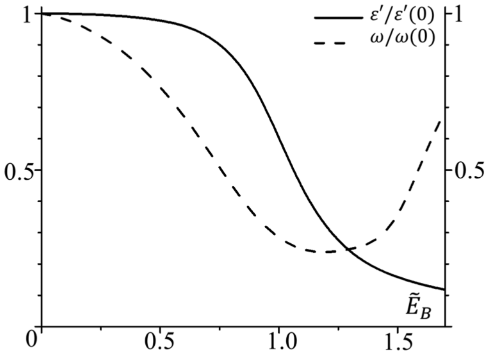

FIG. 6. The dependence of the phase mode relaxation frequency (ω) and the dielectric permittivity (ε') on external bias field ($\tilde{E}_B$). Both values are normalized by the corresponding values in zero bias field [$\varepsilon'(0)$ and $\omega(0)$]. Parameter values: $L/\xi = 7$, $\kappa = 0.3$, and $\tilde{W}_S = 7$ (strong anchoring).

The effect of the bias field on the relaxation frequency is more intriguing. As it is shown in the next section, the bias field renormalizes the elastic constants; it increases the bend and it decreases the splay elastic constant, both renormalizations depend also on the cell thickness and the anchoring strength. At low bias field, the variation of the relaxation frequency (its increase or decrease) with increasing bias field depends on a subtle interplay between the surface and bulk torques.

On the other hand, the increase in relaxation frequency at high bias fields is straightforward to explain. At some bias field, the polar director close to the surface at $x = 0$ aligns along the bias field ($p_x \approx 1$). By increasing the bias field, the region in which the polar director is aligned along the bias field increases, so less and less volume of the cell responds to the AC field. The effect is the same as the effect of changing the cell thickness in zero bias field. If, in the zero bias field, the cell thickness is reduced, the relaxation frequency increases (see Fig. 5 in Ref. [8]).

In Fig. 7 we show the dependence of the phase mode relaxation frequency ω on external bias electric field E_B as a function of the ratio between the elastic constants κ [Fig. 7(a)], cell thickness [Fig. 7(b)], and anchoring strength [Fig. 7(c)].

At weak surface anchoring ($\tilde{W}_S = 1.5$) and in thin cells ($L/\xi = 3$) the relaxation frequency decreases with increasing bias field. The smaller the ratio κ the stronger the decrease [Fig. 7(a)]. However, there exists some critical value (κ_{cr}) above which the relaxation frequency increases with increasing bias field. At a chosen set of parameters we find $\kappa_{\mathrm{cr}} = 1.7$. Numerical calculations show that κ_{cr} decreases with increasing anchoring strength and with decreasing cell thickness.

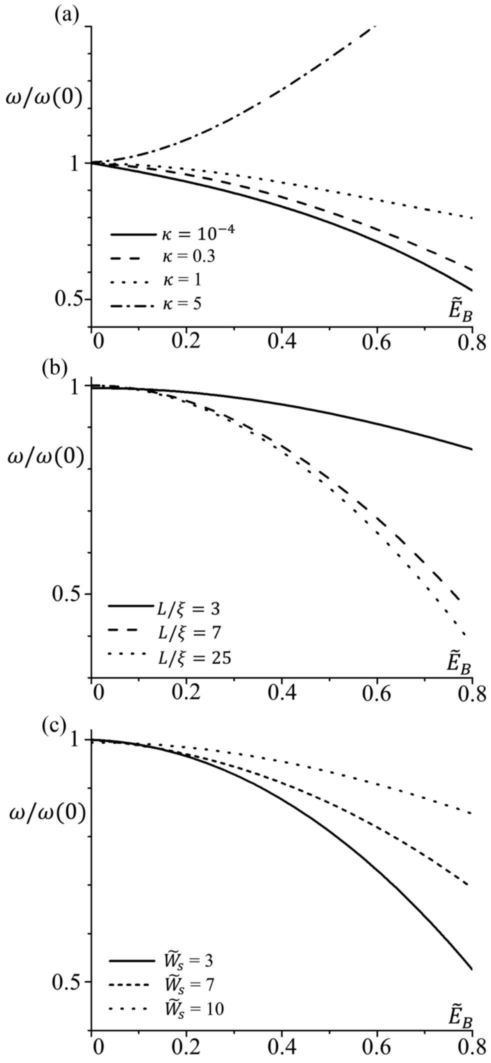

FIG. 7. Phase mode frequency $[\omega/\omega(0)]$ as a function of bias field ($\tilde{E}_B$). (a) The effect of the ratio between the bend and splay elastic constants (κ); $L/\xi = 3$ and $\tilde{W}_S = 1.5$. (b) The effect of the cell thickness (L/ξ); $\kappa = 0.3$ and infinitely strong anchoring. (c) The effect of the polar surface anchoring strength ($\tilde{W}_S$); $\kappa = 0.3$ and $L/\xi = 3$.

At a fixed (strong) surface anchoring and $\kappa = 0.3$ the relaxation frequency decreases with increasing bias field, the decrease is larger in thicker cells [Fig. 7(b)]. At the chosen set of parameters one cannot find the cell thickness below which the relaxation frequency would increase with bias field. As will be shown in Sect. III B, such cell thickness (critical cell thickness) can be found at larger values of κ.

At a constant cell thickness ($L/\xi = 3$) and constant ratio between the bend and splay elastic constant ($\kappa = 0.3$) the relaxation frequency decreases with increasing bias field, the decrease is stronger at weaker surface anchoring [Fig. 7(c)]. At the chosen set of parameters the frequency decreases at all values of anchoring strength, because $L/\xi = 3$ is greater than the critical cell thickness (at infinite anchoring and $\kappa = 0.3$) and $\kappa = 0.3$ is below the critical value (at infinite anchoring and $L/\xi = 3$).

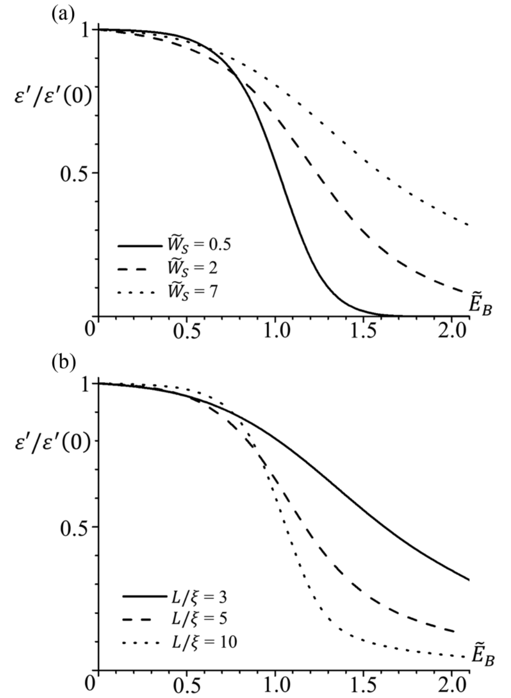

FIG. 8. The dielectric permittivity $[\varepsilon(\omega)]$ as a function of external bias field ($\tilde{E}_B$) for (a) different surface anchoring ($\tilde{W}_S$), $L/\xi = 3$ and $\kappa = 0.3$ and for (b) different cell thicknesses (L/ξ), infinitely strong anchoring, and $\kappa = 0.3$.

Figure 8 shows the dielectric permittivity as a function of bias field for different surface anchorings and cell thicknesses. At a constant cell thickness and κ the decrease in the dielectric permittivity is larger if anchoring is weaker [Fig. 8(a)]. This is expected because at weaker anchoring the polar director structure reaches the uniform structure with $p_x \approx 1$ across the whole cell at lower bias fields. At a given surface anchoring and κ [Fig. 8(b)] the dielectric permittivity decreases with increasing bias field, the decrease is larger in thicker cells.

B. Analytical estimate

The relaxation frequency can be found also analytically in the limit of infinitely strong polar surface anchoring, thin cells, and low external bias field. In thin cells we can approximate the spatial dependence of $p_x(x)$ [or $\varphi(x)$] by a linear function of x (see Fig. 3). If E_B is small, its effect can be considered as a slight harmonic modulation of the structure in zero external field.

The spatial variation of the polar director is expressed as a sum of the equilibrium value $p_0(x)$ at some low bias field E_B and the time-dependent fluctuation part $\delta p(x,t)$ due to the AC field:

$$\vec{p}\,(x) = \vec{p}_0\,(x) + \delta\vec{p}\,(x,t)\,. \tag{20}$$

The x component of the polar director is expressed as

$$p_{0,x}\,(x) = -2\tilde{x} + 1 + \delta p_E \sin(\pi\tilde{x}), \tag{21}$$

where δp_E is the amplitude of the modulation due to external bias field. Since the polar director is a unit vector, the y component of the polar director is obtained as

$p_{0,y} = \sqrt{1 - p_{0,x}^2}$. When Eq. (21) is used in the free energy density [Eq. (8)] and the energy is minimized, we find

$$\delta p_E = \frac{4\tilde{E}_B\,(L/\xi)^2}{\pi((L/\xi)^2 + \pi^2)}. \tag{22}$$

The fluctuation part of the polar director $[\delta\vec{p}(x,t)]$ has the x and y component for which we choose the harmonic ansatz such that the fluctuation amplitude at the surfaces is zero:

$$\delta p_x(x,t) = \delta p_0 \sin\varphi(x) \sin(\pi\tilde{x}) e^{-i\omega t}, \tag{23}$$

$$\delta p_y(x,t) = \delta p_0 \cos\varphi(x) \sin(\pi\tilde{x}) e^{-i\omega t}, \tag{24}$$

where

$$\varphi(x) = \arccos[(p_{0,x}(x)], \tag{25}$$

and ω is the frequency of the external AC field, equal to the relaxation frequency. We insert Eqs. (20) to (24) into Eq. (8) and integrate from 0 to 1 and obtain an expression for the dimensionless free energy, which contains the equilibrium part $(\tilde{F}_{\text{eq}})$ and the part depending on δp_0^2,

$$\tilde{F} = \tilde{F}_{\text{eq}} + A\delta p_0^2, \tag{26}$$

where

$$A = [2.36 + 1.32\kappa + 0.22(L/\xi)^2] + \delta p_E^2[-1.51 + 2.47\kappa - 0.19(L/\xi)^2]. \tag{27}$$

The relaxation frequency is proportional to $AK_{pS}/(\gamma L^2)$ [the factor can be deduced from Eq. (17)], so we finally obtain

$$\frac{\omega}{\omega_\infty} = [1 + (\xi/L)^2(10.7 + 6.0\kappa)] + \delta p_E^2[-0.9 + (\xi/L)^2(-6.9 + 11.2\kappa)], \tag{28}$$

where ω_∞ is the relaxation frequency in bulk and zero bias field (however, note that in bulk, i.e., $L \to \infty$, the approximation is not valid, because we assumed linear variation of the polar director across the cell).

Let us inspect Eq. (28). The first part gives the relaxation frequency in zero bias field. As expected, it increases if the cell thickness decreases and if the bend elastic constant (and thus κ) increases. The second part gives the effect of the bias field on the relaxation frequency. At each cell thickness there exists a critical value of κ above which the frequency increases with increasing bias field. At a given κ there can exist a critical cell thickness below which the frequency will increase with increasing bias field. Figure 9 shows the change of relaxation frequency $\Delta\omega$ with bias field. The analytically obtained results show the same dependence as the ones calculated numerically; however, numerically we showed that such dependencies can be expected also at finite surface anchoring and at a general cell thickness.

C. Comparison with experimental results

Finally, we compare the theoretical results with the experiment. Figure 10 shows the relaxation frequency (ω) and the imaginary part of the dielectric permittivity (ε'') as a function of the voltage applied across the cell (the data is deduced from Fig. 6 in Ref. [8]). We observe that the dependencies of the phase mode frequency and the dielectric permittivity on the voltage across the cell are qualitatively the same as the dependencies of these two quantities on the bias field, obtained by the model. The voltage (U) across the cell is related to the bias field (E_B) as [11,12]

$$U = E_B L - \int_0^L p_x\,dx, \tag{29}$$

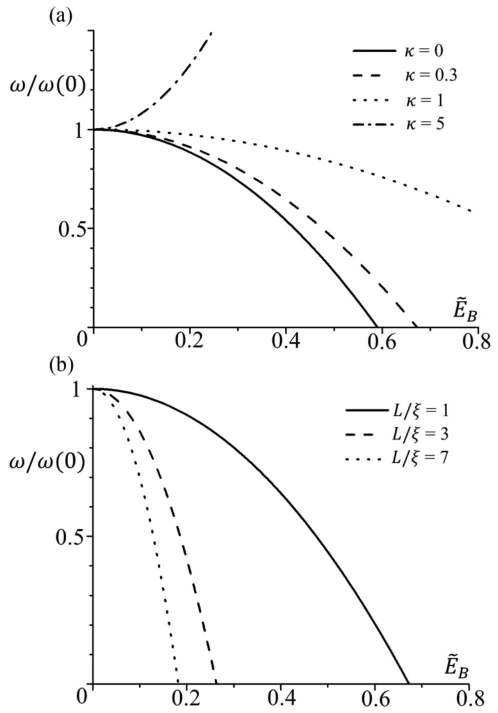

FIG. 9. Analytically calculated change in the relaxation frequency $\omega/\omega(0)$ as a function of bias field $\tilde{E}_B$ at infinitely strong polar surface anchoring. (a) The effect of the ratio between the bend and splay elastic constants (κ); $L/\xi = 3$. (b) The effect of the cell thickness (L/ξ); $\kappa = 0.3$.

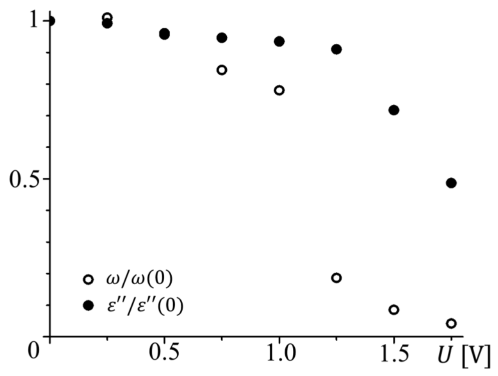

FIG. 10. Experimentally obtained values for the relaxation frequency (ω) (empty circles) and the imaginary part of the dielectric permittivity (ε'') (full circles) as a function of the voltage applied across the cell (U). Both ω and ε'' are normalized by the corresponding value at zero bias field. The data is deduced from Fig. 6 in Ref. [8]; measurements were performed on a 10-μm-thick cell.

where we have neglected the surface dielectric layer, the thickness of which (approximately 50 nm) is usually much thinner that the cell thickness. E_B is the electric field due to the surface charge $\sigma : E_B = \sigma/\varepsilon\varepsilon_0$. This definition includes only the influence of induced dipoles. Due to the reorientation of the permanent dipoles, the electric field inside the cell is further reduced, which significantly reduces the voltage across the cell. By expressing Eq. (29) with dimensionless parameters [Eq. (6)] and using Eq. (14), we find

$$U = U_0(\tilde{E}_B - \langle p_x \rangle), \tag{30}$$

where $U_0 = P_0 L/\varepsilon\varepsilon_0$. By taking $\varepsilon \sim 10$, $P_0 \sim 10^{-3}$ C/m^2, $L \sim 10$ μm, one finds $U_0 \sim 10^2$ V. We are interested in the value of U at which $\omega/\omega(0) \approx 0.5$. Experimentally, in a 10-μm cell, this is at $U \sim 1$ V (see Fig. 10). Theoretically, we thus search for such a set of parameters L/ξ, κ, and $\tilde{W}_S$ at which $(\tilde{E}_B - \langle p_x \rangle)$ at $\omega/\omega(0) \approx 0.5$ is of the order of 10^{-2}.

It is impossible to fit the model to the experimental data, because each point in the graph of $\omega/\omega(0)$ versus $\tilde{E}_B$ is obtained by an extensive set of numerical calculations (see the introduction to Sec. III A). The procedure has to be repeated for each point on the graph at each set of the parameters L/ξ, κ, and $\tilde{W}_S$, varying $\tilde{E}_B$. Considering also the crudeness of the approximation used to calculate the phase mode frequency and the dielectric permittivity, we cannot aim further than the qualitative agreement between the model and the experiment. In addition, a jump in the experimental data for $\omega/\omega(0)$ could be due to the bistability of the surface, the possibility that we have not considered yet. However, we see (Fig. 7) that $\tilde{E}_B - \langle p_x \rangle$ at $\omega/\omega(0) \approx 0.5$ reduces if the surface anchoring strength, cell thickness, and κ decrease. For example, at $L/\xi = 7$, $\kappa = 0.3$, and $\tilde{W}_S = 2$, we find $(\tilde{E}_B - \langle p_x \rangle) = 0.05$. We can thus predict that the surface anchoring is moderately strong and that ξ is of the order of μm rather than 10 μm (as predicted in Ref. [8]).

We also note that the theoretically calculated phase mode frequency starts to increase at high enough bias fields (see Fig. 6). Comparing Figs. 4(c) and 6 we conclude that this effect dominates when the polar director is uniform ($p_x \approx 1$) in approximately 75% of the cell. In such a cell the dielectric response is already very low and we suggest that this is the reason why only a reduction in the relaxation frequency was experimentally observed.

IV. CONCLUSIONS

We have presented a theoretical study of the polar director structure and dielectric response in thin planar cells filled with a bent-core liquid crystal in the ferroelectric smectic-*A* phase (Sm-AP_F). We calculated the effect of the external DC bias electric field on the spatial dependence of the polar director, as a function of the cell thickness, polar anchoring strength, and the ratio between the bend and splay elastic constants. The major part of the paper reports on the study of the dielectric response. Numerical results show that, in general, the phase mode frequency decreases with increasing bias field. Changes in the cell thickness and surface anchoring affect the amount of the decrease. At a given cell thickness there exists a critical value of the ratio between the bend and splay elastic constant, above which the relaxation frequency increases with increasing bias field. The effect of the bias field on the dielectric response was also obtained analytically in the limit of infinitely strong anchoring, thin cells, and low bias field. The analytical results agree well with the numerically obtained results, which enable calculation of the dielectric response at general anchoring strengths, cell thicknesses, and bias fields.

ACKNOWLEDGMENTS

The authors acknowledge the financial support of the Slovenian Research Agency through the research program P1-0055. Useful discussions with Professors Ewa Gorecka, Damian Pociecha, and Noel Clark are greatly appreciated.

[1] T. Niori, T. Sekine, J. Watanabe, T. Furukawa, and H. Takezoe, J. Mater. Chem. **6**, 1231 (1996).
[2] M. Čepič, B. Žekš, and J. Mavri, Mol. Cryst. Liq. Cryst. **328**, 47 (1999).
[3] A. Roy, N. V. Madhusudana, P. Tolédano, and A. M. Figueiredo Neto, Phys. Rev. Lett. **82**, 1466 (1999).
[4] D. Pociecha, E. Gorecka, M. Čepič, N. Vaupotič, and W. Weissflog, Phys. Rev. E **74**, 021702 (2006).
[5] H. Takezoe and Y. Takanishi, Jpn. J. Appl. Phys. **45**, 597 (2006).
[6] R. A. Reddy and C. Tschierske, J. Mater. Chem. **16**, 907 (2006).
[7] R. A. Reddy, C. Zhu, R. Shao, E. Korblova, T. Gong, Y. Shen, E. Garcia, M. A. Glaser, J. E. Maclennan, D. M. Walba, and N. A. Clark, Science **332**, 72 (2011).
[8] L. Guo, E. Gorecka, D. Pociecha, N. Vaupotič, M. Čepič, R. A. Reddy, K. Gornik, F. Araoka, N. A. Clark, D. M. Walba, K. Ishikawa, and H. Takezoe, Phys. Rev. E **84**, 031706 (2011).
[9] C. Zhu, R. Shao, R. A. Reddy, D. Chen, Y. Shen, T. Gong, M. A. Glaser, E. Korblova, P. Rudquist, J. E. Maclennan, D. M. Walba, and N. Clark, J. Am. Chem. Soc. **134**, 9681 (2012).
[10] E. Gorecka, D. Pociecha, F. Araoka, D. R. Link, M. Nakata, J. Thisayukta, Y. Takanishi, K. Ishikawa, J. Watanabe, and H. Takezoe, Phys. Rev. E **62**, R4524 (2000).
[11] Y. Shimbo, E. Gorecka, D. Pociecha, F. Araoka, M. Goto, Y. Takanishi, K. Ishikawa, J. Mieczkowski, K. Gomola, and H. Takezoe, Phys. Rev. Lett. **97**, 113901 (2006).
[12] M. Čopič, J. E. Maclennan, and N. A. Clark, Phys. Rev. E **65**, 021708 (2002).
[13] N. Vaupotič and M. Čopič, Phys. Rev. E **68**, 061705 (2003).
[14] J. E. Maclennan, N. A. Clark, and D. M. Walba, Phys. Rev. E **64**, 031706 (2001).
[15] M. Majumdar, P. Salamon, A. Jákli, J. T. Gleeson, and S. Sprunt, Phys. Rev. E **83**, 031701 (2011).
[16] P. Salamon, N. Éber, J. Seltmann, M. Lehmann, J. T. Gleeson, S. Sprunt, and A. Jákli, Phys. Rev. E **85**, 061704 (2012).

[17] S. Kaur, J. Addis, C. Greco, A. Ferrarini, V. Görtz, J. W. Goodby, and H. F. Gleeson, Phys. Rev. E **86**, 041703 (2012).

[18] S. Kaur, L. Tian, H. Liu, C. Greco, A. Ferrarini, J. Seltmann, M. Lehmann, and H. F. Gleeson, J. Mater. Chem. C **1**, 2416 (2013).

[19] P. G. deGennes and J. Prost, *The Physics of Liquid Crystals*, second edition (Clarendon Press, Oxford, 1993).

[20] P. S. Salter, C. Tschierske, S. J. Elston, and E. P. Raynes, Phys. Rev. E **84**, 031708 (2011).

[21] M. Škarabot, I. Muševič, and R. Blinc, Phys. Rev. E **57**, 6725 (1998).

[22] I. Muševič, R. Blinc, and B. Žekš, *The Physics of Ferroelectric and Antiferroelectric Liquid Crystals* (Word Scientific, Singapore, 2000).